4

Bubble Growth and Collapse

4.1 Introduction

Unlike solid particles or liquid droplets, gas/vapor bubbles can grow or collapse in a flow and in doing so manifest a host of phenomena with technological importance. We devote this chapter to the fundamental dynamics of a growing or collapsing bubble in an infinite domain of liquid that is at rest far from the bubble. Although the assumption of spherical symmetry is violated in several important processes, it is necessary to first develop this baseline. The dynamics of clouds of bubbles or of bubbly flows are treated in later chapters.

4.2 Bubble Growth and Collapse

4.2.1 Rayleigh–Plesset Equation

Consider a spherical bubble of radius, $R(t)$ (where t is time), in an infinite domain of liquid whose temperature and pressure far from the bubble are T_∞ and $p_\infty(t)$ respectively. The temperature, T_∞, is assumed to be a simple constant because temperature gradients are not considered. Conversely, the pressure, $p_\infty(t)$, is assumed to be a known (and perhaps controlled) input that regulates the growth or collapse of the bubble.

Though compressibility of the liquid can be important in the context of bubble collapse, it will, for the present, be assumed that the liquid density, ρ_L, is a constant. Furthermore, the dynamic viscosity, μ_L, is assumed constant and uniform. It will also be assumed that the contents of the bubble are homogeneous and that the temperature, $T_B(t)$, and pressure, $p_B(t)$, within the bubble are always uniform. These assumptions may not be justified in circumstances that will be identified as the analysis proceeds.

The radius of the bubble, $R(t)$, will be one of the primary results of the analysis. As indicated in Figure 4.1, radial position within the liquid will be denoted by the distance, r, from the center of the bubble; the pressure, $p(r, t)$, radial outward velocity, $u(r, t)$, and temperature, $T(r, t)$, within the liquid will be so designated. Conservation

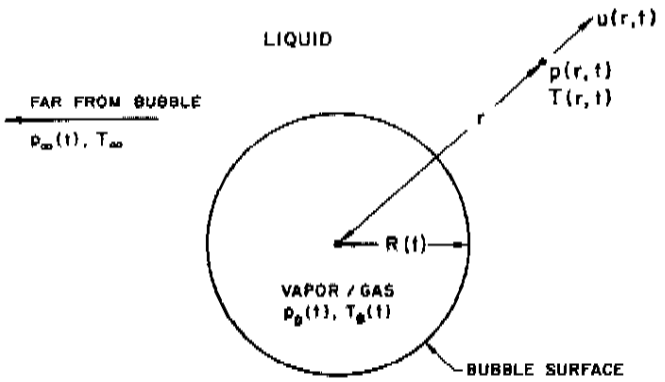

Figure 4.1. Schematic of a spherical bubble in an infinite liquid.

of mass requires that

$$u(r,t) = \frac{F(t)}{r^2}, \tag{4.1}$$

where $F(t)$ is related to $R(t)$ by a kinematic boundary condition at the bubble surface. In the idealized case of zero mass transport across this interface, it is clear that $u(R,t) = dR/dt$ and hence

$$F(t) = R^2 \frac{dR}{dt}. \tag{4.2}$$

This is often a good approximation even when evaporation or condensation is occurring at the interface (Brennen 1995) provided the vapor density is much smaller than the liquid density.

Assuming a Newtonian liquid, the Navier–Stokes equation for motion in the r direction,

$$-\frac{1}{\rho_L}\frac{\partial p}{\partial r} = \frac{\partial u}{\partial t} + u\frac{\partial u}{\partial r} - \nu_L\left\{\frac{1}{r^2}\frac{\partial}{\partial r}\left(r^2\frac{\partial u}{\partial r}\right) - \frac{2u}{r^2}\right\} \tag{4.3}$$

yields, after substituting for u from $u = F(t)/r^2$, the following:

$$-\frac{1}{\rho_L}\frac{\partial p}{\partial r} = \frac{1}{r^2}\frac{dF}{dt} - \frac{2F^2}{r^5}. \tag{4.4}$$

Note that the viscous terms vanish; indeed, the only viscous contribution to the Rayleigh–Plesset Eq. (4.8) comes from the dynamic boundary condition at the bubble surface. Equation (4.4) can be integrated to give the following:

$$\frac{p - p_\infty}{\rho_L} = \frac{1}{r}\frac{dF}{dt} - \frac{1}{2}\frac{F^2}{r^4} \tag{4.5}$$

after application of the condition $p \to p_\infty$ as $r \to \infty$.

To complete this part of the analysis, a dynamic boundary condition on the bubble surface must be constructed. For this purpose consider a control volume consisting of

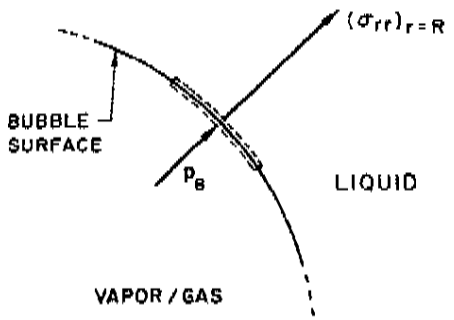

Figure 4.2. Portion of the spherical bubble surface.

a small, infinitely thin lamina containing a segment of interface (Figure 4.2). The net force on this lamina in the radially outward direction per unit area is as follows:

$$(\sigma_{rr})_{r=R} + p_B - \frac{2S}{R} \tag{4.6}$$

or, because $\sigma_{rr} = -p + 2\mu_L \partial u/\partial r$, the force per unit area is as follows:

$$p_B - (p)_{r=R} - \frac{4\mu_L}{R}\frac{dR}{dt} - \frac{2S}{R}. \tag{4.7}$$

In the absence of mass transport across the boundary (evaporation or condensation) this force must be zero, and substitution of the value for $(p)_{r=R}$ from Eq. (4.5) with $F = R^2 dR/dt$ yields the following generalized Rayleigh–Plesset equation for bubble dynamics:

$$\frac{p_B(t) - p_\infty(t)}{\rho_L} = R\frac{d^2R}{dt^2} + \frac{3}{2}\left(\frac{dR}{dt}\right)^2 + \frac{4\nu_L}{R}\frac{dR}{dt} + \frac{2S}{\rho_L R}. \tag{4.8}$$

Given $p_\infty(t)$ this represents an equation that can be solved to find $R(t)$ provided $p_B(t)$ is known. In the absence of the surface tension and viscous terms, it was first derived and used by Rayleigh (1917). Plesset (1949) first applied the equation to the problem of traveling cavitation bubbles.

4.2.2 Bubble Contents

In addition to the Rayleigh–Plesset equation, considerations of the bubble contents are necessary. To be fairly general, it is assumed that the bubble contains some quantity of noncondensable gas whose partial pressure is p_{G_0} at some reference size, R_0, and temperature, T_∞. Then, if there is no appreciable mass transfer of gas to or from the liquid, it follows that

$$p_B(t) = p_V(T_B) + p_{G_0}\left(\frac{T_B}{T_\infty}\right)\left(\frac{R_0}{R}\right)^3. \tag{4.9}$$

In some cases this last assumption is not justified, and it is necessary to solve a mass transport problem for the liquid in a manner similar to that used for heat diffusion (see Section 4.3.4).

It remains to determine $T_B(t)$. This is not always necessary because, under some conditions, the difference between the unknown T_B and the known T_∞ is negligible. But there are also circumstances in which the temperature difference, $(T_B(t) - T_\infty)$, is important and the effects caused by this difference dominate the bubble dynamics. Clearly the temperature difference, $(T_B(t) - T_\infty)$, leads to a different vapor pressure, $p_V(T_B)$, than would occur in the absence of such thermal effects, and this alters the growth or collapse rate of the bubble. It is therefore instructive to substitute Eq. (4.9) into Eq. (4.8) and thereby write the Rayleigh–Plesset equation in the following general form:

$$\underset{(1)}{\frac{p_V(T_\infty) - p_\infty(t)}{\rho_L}} + \underset{(2)}{\frac{p_V(T_B) - p_V(T_\infty)}{\rho_L}} + \underset{(3)}{\frac{p_{G_0}}{\rho_L}\left(\frac{T_B}{T_\infty}\right)\left(\frac{R_0}{R}\right)^3} = \underset{(4)}{R\frac{d^2R}{dt^2}} + \underset{(5)}{\frac{3}{2}\left(\frac{dR}{dt}\right)^2} + \underset{(5)}{\frac{4\nu_L}{R}\frac{dR}{dt}} + \underset{(6)}{\frac{2S}{\rho_L R}}. \tag{4.10}$$

The first term, (1), is the instantaneous tension or driving term determined by the conditions far from the bubble. The second term, (2), is referred to as the *thermal term*, and it will be seen that very different bubble dynamics can be expected depending on the magnitude of this term. When the temperature difference is small, it is convenient to use a Taylor expansion in which only the first derivative is retained to evaluate

$$\frac{p_V(T_B) - p_V(T_\infty)}{\rho_L} = A(T_B - T_\infty) \tag{4.11}$$

where the quantity A may be evaluated from the following:

$$A = \frac{1}{\rho_L}\frac{dp_V}{dT} = \frac{\rho_V(T_\infty)\mathcal{L}(T_\infty)}{\rho_L T_\infty} \tag{4.12}$$

using the Clausius–Clapeyron relation, $\mathcal{L}(T_\infty)$ being the latent heat of vaporization at the temperature T_∞. It is consistent with the Taylor expansion approximation to evaluate ρ_V and $\mathcal{L}$ at the known temperature T_∞. It follows that, for small temperature differences, term (2) in Eq. (4.10) is given by $A(T_B - T_\infty)$.

The degree to which the bubble temperature, T_B, departs from the remote liquid temperature, T_∞, can have a major effect on the bubble dynamics, and it is necessary to discuss how this departure might be evaluated. The determination of $(T_B - T_\infty)$ requires two steps. First, it requires the solution of the heat diffusion equation,

$$\frac{\partial T}{\partial t} + \frac{dR}{dt}\left(\frac{R}{r}\right)^2\frac{\partial T}{\partial r} = \frac{\mathcal{D}_L}{r^2}\frac{\partial}{\partial r}\left(r^2\frac{\partial T}{\partial r}\right), \tag{4.13}$$

to determine the temperature distribution, $T(r, t)$, within the liquid ($\mathcal{D}_L$ is the thermal diffusivity of the liquid). Second, it requires an energy balance for the bubble. The

heat supplied to the interface from the liquid is

$$4\pi R^2 k_L \left(\frac{\partial T}{\partial r}\right)_{r=R}, \tag{4.14}$$

where k_L is the thermal conductivity of the liquid. Assuming that all of this is used for vaporization of the liquid (this neglects the heat used for heating or cooling the existing bubble contents, which is negligible in many cases), one can evaluate the mass rate of production of vapor and relate it to the known rate of increase of the volume of the bubble. This yields

$$\frac{dR}{dt} = \frac{k_L}{\rho_V \mathcal{L}} \left(\frac{\partial T}{\partial r}\right)_{r=R}, \tag{4.15}$$

where k_L, ρ_V, and $\mathcal{L}$ should be evaluated at $T = T_B$. If, however, $T_B - T_\infty$ is small, it is consistent with the linear analysis described earlier to evaluate these properties at $T = T_\infty$.

The nature of the thermal effect problem is now clear. The thermal term in the Rayleigh–Plesset Eq. (4.10) requires a relation between $(T_B(t) - T_\infty)$ and $R(t)$. The energy balance Eq. (4.15) yields a relation between $(\partial T/\partial r)_{r=R}$ and $R(t)$. The final relation between $(\partial T/\partial r)_{r=R}$ and $(T_B(t) - T_\infty)$ requires the solution of the heat diffusion equation. It is this last step that causes considerable difficulty due to the evident nonlinearities in the heat diffusion equation; no exact analytic solution exists. However, the solution of Plesset and Zwick (1952) provides a useful approximation for many purposes. This solution is confined to cases in which the thickness of the thermal boundary layer, δ_T, surrounding the bubble is small compared with the radius of the bubble, a restriction that can be roughly represented by the identity

$$R \gg \delta_T \approx (T_\infty - T_B) \Big/ \left(\frac{\partial T}{\partial r}\right)_{r=R}. \tag{4.16}$$

The Plesset–Zwick result is that

$$T_\infty - T_B(t) = \left(\frac{\mathcal{D}_L}{\pi}\right)^{\frac{1}{2}} \int_0^t \frac{[R(x)]^2 \left(\frac{\partial T}{\partial r}\right)_{r=R(x)} dx}{\left\{\int_x^t [R(y)]^4 dy\right\}^{\frac{1}{2}}}, \tag{4.17}$$

where x and y are dummy time variables. Using Eq. (4.15) this can be written as follows:

$$T_\infty - T_B(t) = \frac{\mathcal{L}\rho_V}{\rho_L c_{pL} \mathcal{D}_L^{\frac{1}{2}}} \left(\frac{1}{\pi}\right)^{\frac{1}{2}} \int_0^t \frac{[R(x)]^2 \frac{dR}{dx} dx}{\left[\int_x^t R^4(y) dy\right]^{\frac{1}{2}}}. \tag{4.18}$$

This can be directly substituted into the Rayleigh–Plesset equation to generate a complicated integro-differential equation for $R(t)$. However, for present purposes it is more instructive to confine our attention to regimes of bubble growth or collapse that

can be approximated by the following relation:

$$R = R^* t^n, \tag{4.19}$$

where R^* and n are constants. Then Eq. (4.18) reduces to the following:

$$T_\infty - T_B(t) = \frac{\mathcal{L}\rho_V}{\rho_L c_{PL} \mathcal{D}_L^{\frac{1}{2}}} R^* t^{n-\frac{1}{2}} C(n) \tag{4.20}$$

where the constant

$$C(n) = n\left(\frac{4n+1}{\pi}\right)^{\frac{1}{2}} \int_0^1 \frac{z^{3n-1}dz}{(1-z^{4n+1})^{\frac{1}{2}}} \tag{4.21}$$

and is of the order unity for most values of n of practical interest ($0 < n < 1$ in the case of bubble growth). Under these conditions the linearized form of the thermal term, (2), in the Rayleigh–Plesset Eq. (4.10) as given by Eqs. (4.11) and (4.12) becomes the following:

$$(T_B - T_\infty)\frac{\rho_V \mathcal{L}}{\rho_L T_\infty} = -\Sigma(T_\infty) C(n) R^* t^{n-\frac{1}{2}}, \tag{4.22}$$

where the thermodynamic parameter is defined as follows:

$$\Sigma(T_\infty) = \frac{\mathcal{L}^2 \rho_V^2}{\rho_L^2 c_{PL} T_\infty \mathcal{D}_L^{\frac{1}{2}}}. \tag{4.23}$$

In Section 4.3.1 it will be seen that this parameter, Σ, whose units are meters per second to the 3/2 power, is crucially important in determining the bubble dynamic behavior.

4.2.3 In the Absence of Thermal Effects; Bubble Growth

First we consider some of the characteristics of bubble dynamics in the absence of any significant thermal effects. This kind of bubble dynamic behavior is termed *inertially controlled* to distinguish it from the *thermally controlled* behavior discussed later. Under these circumstances the temperature in the liquid is assumed uniform and term (2) in the Rayleigh–Plesset Eq. (4.10) is zero.

For simplicity, it is assumed that the behavior of the gas in the bubble is polytropic so that

$$p_G = p_{Go}\left(\frac{R_o}{R}\right)^{3k}, \tag{4.24}$$

where k is approximately constant. Clearly $k = 1$ implies a constant bubble temperature and $k = \gamma$ would model adiabatic behavior. It should be understood that accurate evaluation of the behavior of the gas in the bubble requires the solution of the mass,

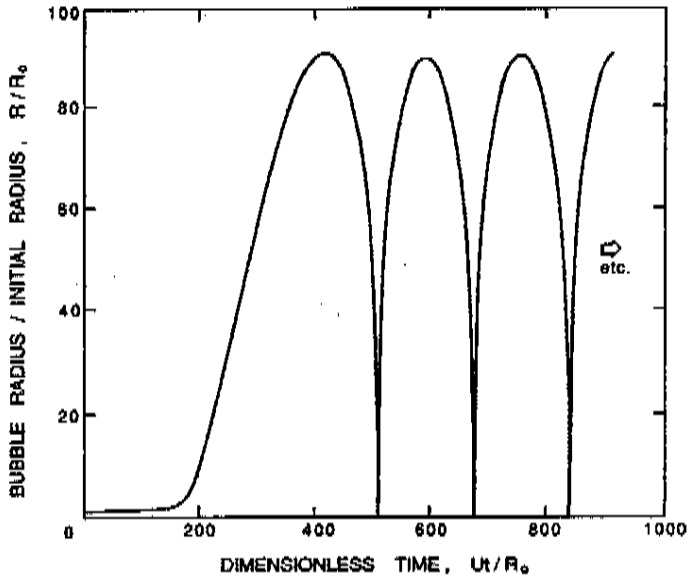

Figure 4.3. Typical solution of the Rayleigh–Plesset equation for a spherical bubble. The nucleus of radius, R_0, enters a low-pressure region at a dimensionless time of 0 and is convected back to the original pressure at a dimensionless time of 500. The low-pressure region is sinusoidal and symmetric about 250.

momentum, and energy equations for the bubble contents combined with appropriate boundary conditions that will include a thermal boundary condition at the bubble wall.

With these assumptions the Rayleigh–Plesset equation becomes

$$\frac{p_V(T_\infty) - p_\infty(t)}{\rho_L} + \frac{p_{G0}}{\rho_L}\left(\frac{R_0}{R}\right)^{3k} = R\frac{d^2R}{dt^2} + \frac{3}{2}\left(\frac{dR}{dt}\right)^2 + \frac{4\nu_L}{R}\frac{dR}{dt} + \frac{2S}{\rho_L R} \tag{4.25}$$

Equation (4.25) without the viscous term was first derived and used by Noltingk and Neppiras (1950, 1951); the viscous term was investigated first by Poritsky (1952).

Equation (4.25) can be readily integrated numerically to find $R(t)$ given the input $p_\infty(t)$, the temperature T_∞, and the other constants. Initial conditions are also required and, in the context of cavitating flows, it is appropriate to assume that the bubble begins as a microbubble of radius R_0 in equilibrium at $t = 0$ at a pressure $p_\infty(0)$ so that

$$p_{G0} = p_\infty(0) - p_V(T_\infty) + \frac{2S}{R_0} \tag{4.26}$$

and that $dR/dt|_{t=0} = 0$. A typical solution for Eq. (4.25) under these conditions is shown in Figure 4.3; the bubble in this case experiences a pressure, $p_\infty(t)$, that first decreases below $p_\infty(0)$ and then recovers to its original value. The general features of this solution are characteristic of the response of a bubble as it passes through any low pressure region; they also reflect the strong nonlinearity of Eq. (4.25). The growth is fairly smooth and the maximum size occurs after the minimum pressure.

The collapse process is quite different. The bubble collapses catastrophically, and this is followed by successive rebounds and collapses. In the absence of dissipation mechanisms such as viscosity these rebounds would continue indefinitely without attenuation.

Analytic solutions to Eq. (4.25) are limited to the case of a step function change in p_∞. Nevertheless, these solutions reveal some of the characteristics of more general pressure histories, $p_\infty(t)$, and are therefore valuable to document. With a constant value of $p_\infty(t > 0) = p_\infty^*$, Eq. (4.25) is integrated by multiplying through by $2R^2 dR/dt$ and forming time derivatives. Only the viscous term cannot be integrated in this way, and what follows is confined to the inviscid case. After integration, application of the initial condition $(dR/dt)_{t=0} = 0$ yields the following:

$$\left(\frac{dR}{dt}\right)^2 = \frac{2(p_V - p_\infty^*)}{3\rho_L}\left\{1 - \frac{R_o^3}{R^3}\right\} + \frac{2p_{Go}}{3\rho_L(1-k)}\left\{\frac{R_o^{3k}}{R^{3k}} - \frac{R_o^3}{R^3}\right\} - \frac{2S}{\rho_L R}\left\{1 - \frac{R_o^2}{R^2}\right\} \tag{4.27}$$

where, in the case of isothermal gas behavior, the term involving p_{Go} becomes

$$2\frac{p_{Go}}{\rho_L}\frac{R_o^3}{R^3}\ln\left(\frac{R_o}{R}\right). \tag{4.28}$$

By rearranging Eq. (4.27) it follows that

$$t = R_o \int_0^{R/R_o} \left\{\frac{2\left(p_V - p_\infty^*\right)\left(1 - x^{-3}\right)}{3\rho_L} + \frac{2p_{Go}\left(x^{-3k} - x^{-3}\right)}{3\left(1-k\right)\rho_L} - \frac{2S\left(1 - x^{-2}\right)}{\rho_L R_o x}\right\}^{-\frac{1}{2}} dx, \tag{4.29}$$

where, in the case $k = 1$, the gas term is replaced by the following:

$$\frac{2p_{Go}}{x^3}\ln x. \tag{4.30}$$

This integral can be evaluated numerically to find $R(t)$, albeit indirectly.

Consider first the characteristic behavior for bubble growth that this solution exhibits when $p_\infty^* < p_\infty(0)$. Equation (4.27) shows that the asymptotic growth rate for $R \gg R_o$ is given by the following:

$$\frac{dR}{dt} \to \left\{\frac{2}{3}\frac{\left(p_V - p_\infty^*\right)}{\rho_L}\right\}^{\frac{1}{2}}. \tag{4.31}$$

Thus, following an initial period of acceleration, the velocity of the interface is relatively constant. It should be emphasized that Eq. (4.31) implies explosive growth of the bubble, in which the volume displacement is increasing like t^3.

4.2.4 In the Absence of Thermal Effects; Bubble Collapse

Now contrast the behavior of a bubble caused to collapse by an increase in p_∞ to p_∞^*. In this case when $R \ll R_o$ Eq. (4.27) yields the following:

$$\frac{dR}{dt} \to -\left(\frac{R_o}{R}\right)^{\frac{3}{2}} \left\{ \frac{2(p_\infty^* - p_V)}{3\rho_L} + \frac{2S}{\rho_L R_o} - \frac{2p_{Go}}{3(k-1)\rho_L} \left(\frac{R_o}{R}\right)^{3(k-1)} \right\}^{\frac{1}{2}}, \quad (4.32)$$

where, in the case of $k = 1$, the gas term is replaced by $2p_{Go} \ln(R_o/R)/\rho_L$. However, most bubble collapse motions become so rapid that the gas behavior is much closer to adiabatic than isothermal, and we will therefore assume $k \neq 1$.

For a bubble with a substantial gas content the asymptotic collapse velocity given by Eq. (4.32) will not be reached and the bubble will simply oscillate about a new, but smaller, equilibrium radius. Conversely, when the bubble contains very little gas, the inward velocity will continually increase (like $R^{-3/2}$) until the last term within the curly brackets reaches a magnitude comparable with the other terms. The collapse velocity will then decrease and a minimum size given by the following:

$$R_{min} = R_o \left\{ \frac{1}{(k-1)} \frac{p_{Go}}{\left(p_\infty^* - p_V - p_{Go} + 3S/R_o\right)} \right\}^{\frac{1}{3(k-1)}} \quad (4.33)$$

will be reached, following which the bubble will rebound. Note that, if p_{Go} is small, R_{min} could be very small indeed. The pressure and temperature of the gas in the bubble at the minimum radius are then given by p_m and T_m where

$$p_m = p_{Go} \left\{ (k-1) \left(p_\infty^* - p_V - p_{Go} + 3S/R_o\right)/p_{Go} \right\}^{k/(k-1)} \quad (4.34)$$

$$T_m = T_o \left\{ (k-1) \left(p_\infty^* - p_V - p_{Go} + 3S/R_o\right)/p_{Go} \right\}. \quad (4.35)$$

We comment later on the magnitudes of these temperatures and pressures (see Sections 5.2.2 and 5.3.3).

The case of zero gas content presents a special albeit somewhat hypothetical problem, because apparently the bubble will reach zero size and at that time have an infinite inward velocity. In the absence of both surface tension and gas content, Rayleigh (1917) was able to integrate Eq. (4.29) to obtain the time, t_{tc}, required for total collapse from $R = R_o$ to $R = 0$:

$$t_{tc} = 0.915 \left(\frac{\rho_L R_o^2}{p_\infty^* - p_V} \right)^{\frac{1}{2}}. \quad (4.36)$$

It is important at this point to emphasize that although the results for bubble growth in Section 4.2.3 are quite practical, the results for bubble collapse may be quite misleading. Apart from the neglect of thermal effects, the analysis was based on two other assumptions that may be violated during collapse. Later it is shown that the final stages of collapse may involve such high velocities (and pressures) that the assumption of liquid incompressibility is no longer appropriate. But, perhaps more

important, it transpires (see Section 5.2.3) that a collapsing bubble loses its spherical symmetry in ways that can have important engineering consequences.

4.2.5 Stability of Vapor/Gas Bubbles

Apart from the characteristic bubble growth and collapse processes discussed in the last section, it is also important to recognize that the following equilibrium condition

$$p_V - p_\infty + p_{Ge} - \frac{2S}{R_e} = 0 \tag{4.37}$$

may not always represent a *stable* equilibrium state at $R = R_e$ with a partial pressure of gas p_{Ge}.

Consider a small perturbation in the size of the bubble from $R = R_e$ to $R = R_e(1 + \epsilon)$, $\epsilon \ll 1$, and the response resulting from the Rayleigh–Plesset equation. Care must be taken to distinguish two possible cases:

(1) The partial pressure of the gas remains the same at p_{Ge}.
(2) The mass of gas in the bubble and its temperature, T_B, remain the same.

From a practical point of view the Case (1) perturbation is generated over a length of time sufficient to allow adequate mass diffusion in the liquid so that the partial pressure of gas is maintained at the value appropriate to the concentration of gas dissolved in the liquid. Conversely, Case (2) is considered to take place too rapidly for significant gas diffusion. It follows that in Case (1) the gas term in the Rayleigh–Plesset Eq. (4.25) is p_{Ge}/ρ_L, whereas in Case (2) it is $p_{Ge}R_e^{3k}/\rho_L R^{3k}$. If n is defined as zero for Case (1) and $n = 1$ for Case (2) then substitution of $R = R_e(1 + \epsilon)$ into the Rayleigh–Plesset equation yields the following:

$$R\frac{d^2R}{dt^2} + \frac{3}{2}\left(\frac{dR}{dt}\right)^2 + \frac{4\nu_L}{R}\frac{dR}{dt} = \frac{\epsilon}{\rho_L}\left\{\frac{2S}{R_e} - 3nkp_{Ge}\right\}. \tag{4.38}$$

Note that the right-hand side has the same sign as ϵ if

$$\frac{2S}{R_e} > 3nkp_{Ge} \tag{4.39}$$

and a different sign if the reverse holds. Therefore, if the above inequality holds, the left-hand side of Eq. (4.38) implies that the velocity and/or acceleration of the bubble radius has the same sign as the perturbation, and hence the equilibrium is *unstable* because the resulting motion will cause the bubble to deviate further from $R = R_e$. Conversely, the equilibrium is stable if $np_{Ge} > 2S/3R_e$.

First consider Case (1) which must always be *unstable* because the inequality 4.39 always holds if $n = 0$. This is simply a restatement of the fact (discussed in Section 4.3.4) that, if one allows time for mass diffusion, then all bubbles will either grow or shrink indefinitely.

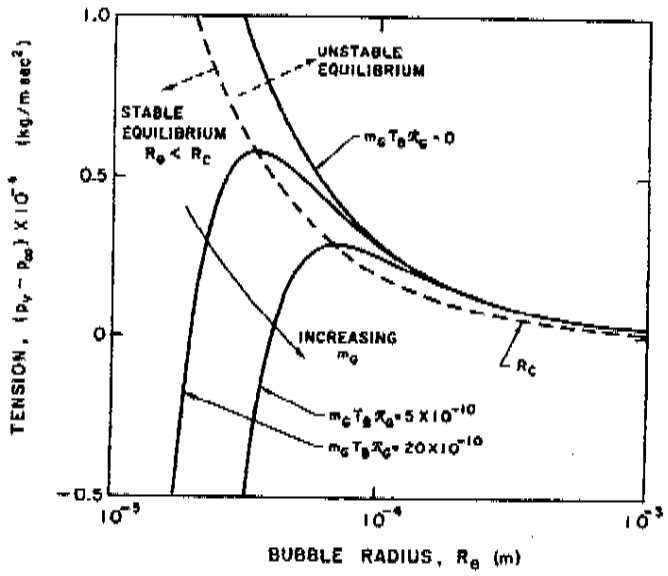

Figure 4.4. Stable and unstable bubble equilibrium radii as a function of the tension for various masses of gas in the bubble. Stable and unstable conditions are separated by the dotted line. Adapted from Daily and Johnson (1956).

Case (2) is more interesting because, in many of the practical engineering situations, pressure levels change over a period of time that is short compared with the time required for significant gas diffusion. In this case a bubble in stable equilibrium requires the following:

$$p_{Ge} = \frac{m_G T_B \mathcal{R}_G}{\frac{4}{3}\pi R_e^3} > \frac{2S}{3kR_e}, \tag{4.40}$$

where m_G is the mass of gas in the bubble and $\mathcal{R}_G$ is the gas constant. Indeed for a *given* mass of gas there exists a critical bubble size, R_c, where

$$R_c = \left\{ \frac{9km_G T_B \mathcal{R}_G}{8\pi S} \right\}^{1/2}. \tag{4.41}$$

This critical radius was first identified by Blake (1949) and Neppiras and Noltingk (1951) and is often referred to as the Blake critical radius. All bubbles of radius $R_e < R_c$ can exist in stable equilibrium, whereas all bubbles of radius $R_e > R_c$ must be unstable. This critical size could be reached by decreasing the ambient pressure from p_∞ to the critical value, $p_{\infty c}$, where from Eqs. (4.41) and (4.37) it follows that

$$p_{\infty c} = p_V - \frac{4S}{3}\left\{ \frac{8\pi S}{9km_G T_B \mathcal{R}_G} \right\}^{\frac{1}{2}}, \tag{4.42}$$

which is often called the Blake threshold pressure.

The isothermal case ($k = 1$) is presented graphically in Figure 4.4, where the solid lines represent equilibrium conditions for a bubble of size R_e plotted against the

tension $(p_V - p_\infty)$ for various fixed masses of gas in the bubble and a fixed surface tension. The critical radius for any particular m_G corresponds to the maximum in each curve. The locus of the peaks is the graph of R_c values and is shown by the dashed line whose equation is $(p_V - p_\infty) = 4S/3R_c$. The region to the right of the dashed line represents unstable equilibrium conditions. This graphical representation was used by Daily and Johnson (1956) and is useful in visualizing the quasistatic response of a bubble when subjected to a decreasing pressure. Starting in the fourth quadrant under conditions in which the ambient pressure, $p_\infty > p_V$, and, assuming the mass of gas in the bubble is constant, the radius, R_c, will first increase as $(p_V - p_\infty)$ increases. The bubble will pass through a series of stable equilibrium states until the particular critical pressure corresponding to the maximum is reached. Any slight decrease in p_∞ below the value corresponding to this point will result in explosive cavitation growth regardless of whether p_∞ is further decreased. In the context of cavitation nucleation (Brennen 1995), it is recognized that a system consisting of small bubbles in a liquid can sustain a *tension* in the sense that it may be in equilibrium at liquid pressures below the vapor pressure. Due to surface tension, the maximum tension, $(p_V - p_\infty)$, that such a system could sustain would be $2S/R$. However, it is clear from the above analysis that stable equilibrium conditions do not exist in the range

$$\frac{4S}{3R} < (p_V - p_\infty) < \frac{2S}{R} \tag{4.43}$$

and therefore the maximum tension should be given by $4S/3R$ rather than $2S/R$.

4.3 Thermal Effects

4.3.1 Thermal Effects on Growth

In Sections 4.2.3 through 4.2.5 some of the characteristics of bubble dynamics in the absence of thermal effects were explored. It is now necessary to examine the regime of validity of those analyses. First we evaluate the magnitude of the thermal term (2) in Eq. (4.10) [see also Eq. (4.22)] that was neglected to produce Eq. (4.25).

First examine the case of bubble growth. The asymptotic growth rate given by Eq. (4.31) is constant and hence in the characteristic case of a constant p_∞, terms (1), (3), (4), (5), and (6) in Eq. (4.10) are all either constant or diminishing in magnitude as time progresses. Note that a constant, asymptotic growth rate corresponds to the case

$$n = 1; \quad R^* = \left\{2\left(p_V - p_\infty^*\right)/3\rho_L\right\}^{\frac{1}{2}} \tag{4.44}$$

in Eq. (4.19). Consequently, according to Eq. (4.22), the thermal term (2) in its linearized form for small $(T_\infty - T_B)$ is given by the following:

$$\text{term (2)} = \Sigma(T_\infty)C(1)R^* t^{\frac{1}{2}}. \tag{4.45}$$

Under these conditions, even if the thermal term is initially negligible, it will gain in magnitude relative to all the other terms and will ultimately affect the growth in a major way. Parenthetically it should be added that the Plesset–Zwick assumption of a small thermal boundary layer thickness, δ_T, relative to R can be shown to hold throughout the inertially controlled growth period because δ_T increases like $(\mathcal{D}_L t)^{\frac{1}{2}}$, whereas R is increasing linearly with t. Only under circumstances of very slow growth might the assumption be violated.

Using the relation 4.45, one can therefore define a critical time, t_{c1} (called the first critical time), during growth when the order of magnitude of term (2) in Eq. (4.10) becomes equal to the order of magnitude of the retained terms, as represented by $(dR/dt)^2$. This first critical time is given by the following:

$$t_{c1} = \frac{(p_V - p^*_\infty)}{\rho_L} \cdot \frac{1}{\Sigma^2}, \tag{4.46}$$

where the constants of the order of unity have been omitted for clarity. Thus t_{c1} depends not only on the tension $(p_V - p^*_\infty)/\rho_L$ but also on $\Sigma(T_\infty)$, a purely thermophysical quantity that is a function only of the liquid temperature. Recalling Eq. (4.23),

$$\Sigma(T) = \frac{\mathcal{L}^2 \rho_V^2}{\rho_L^2 c_{PL} T_\infty \mathcal{D}_L^{\frac{1}{2}}}, \tag{4.47}$$

it can be anticipated that Σ^2 will change by many, many orders of magnitude in a given liquid as the temperature T_∞ is varied from the triple point to the critical point because Σ^2 is proportional to $(\rho_V/\rho_L)^4$. As a result the critical time, t_{c1}, will vary by many orders of magnitude. Some values of Σ for a number of liquids are plotted in Figure 4.5 as a function of the reduced temperature T/T_C. As an example, consider a typical cavitating flow experiment in a water tunnel with a tension of the order of 10^4 kg/m s^2. Because water at 20°C has a value of Σ of about 1 m/s$^{\frac{3}{2}}$, the first critical time is of the order of 10 s, which is very much longer than the time of growth of bubbles. Hence the bubble growth occurring in this case is unhindered by thermal effects; it is *inertially controlled* growth. Conversely, if the tunnel water were heated to 100°C or, equivalently, one observed bubble growth in a pot of boiling water at superheat of 2°K, then because $\Sigma \approx 10^3$ m/s$^{\frac{3}{2}}$ at 100°C the first critical time would be 10 μs. Thus virtually all the bubble growth observed would be *thermally controlled.*

4.3.2 Thermally Controlled Growth

When the first critical time is exceeded it is clear that the relative importance of the various terms in the Rayleigh–Plesset Eq. (4.10), will change. The most important terms become the driving term (1) and the thermal term (2), whose magnitude is much larger than that of the inertial terms (4). Hence if the tension $(p_V - p^*_\infty)$ remains constant, then the solution using the form of Eq. (4.22) for the thermal term must have

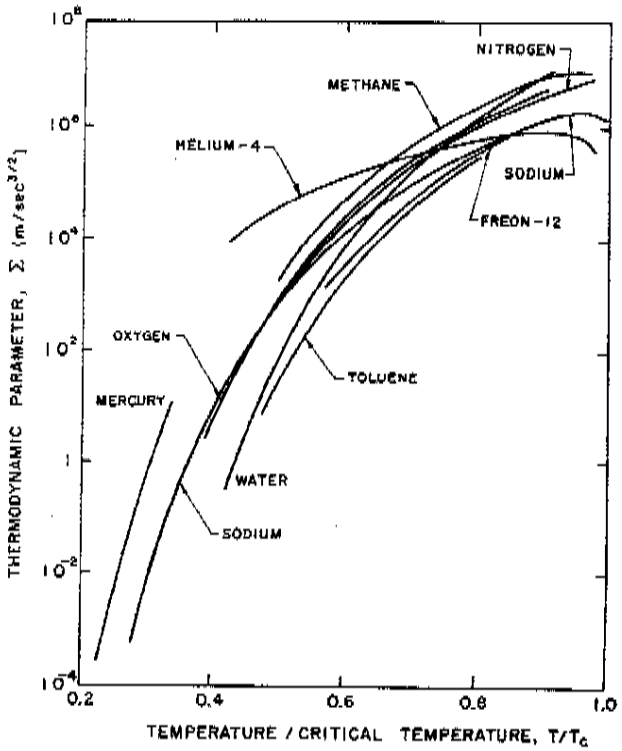

Figure 4.5. Values of the thermodynamic parameter, Σ, for various saturated liquids as a function of the reduced temperature, T/T_C.

$n = \frac{1}{2}$ and the asymptotic behavior is as follows:

$$R = \frac{(p_V - p_\infty^*)\, t^{\frac{1}{2}}}{\rho_L \Sigma(T_\infty) C(\frac{1}{2})} \quad or \quad n = \frac{1}{2}; \quad R^* = \frac{(p_V - p_\infty^*)}{\rho_L \Sigma(T_\infty) C(\frac{1}{2})}. \tag{4.48}$$

Consequently, as time proceeds, the inertial, viscous, gaseous, and surface tension terms in the Rayleigh–Plesset equation all rapidly decline in importance. In terms of the superheat, ΔT, rather than the tension

$$R = \frac{1}{2C(\frac{1}{2})} \frac{\rho_L c_{PL} \Delta T}{\rho_V \mathcal{L}} (\mathcal{D}_L t)^{\frac{1}{2}}, \tag{4.49}$$

where the group $\rho_L c_{PL} \Delta T / \rho_V \mathcal{L}$ is termed the Jakob number in the context of pool boiling and $\Delta T = T_w - T_\infty$, T_w being the wall temperature. We note here that this section addresses only the issues associated with bubble growth in the liquid bulk. The presence of a nearby wall (as is the case in most boiling) causes details and complications, the discussion of which is delayed until Chapter 6.

The result, Eq. (4.48), demonstrates that the rate of growth of the bubble decreases substantially after the first critical time, t_{c1}, is reached and that R subsequently increases like $t^{\frac{1}{2}}$ instead of t. Moreover, because the thermal boundary layer also increases like

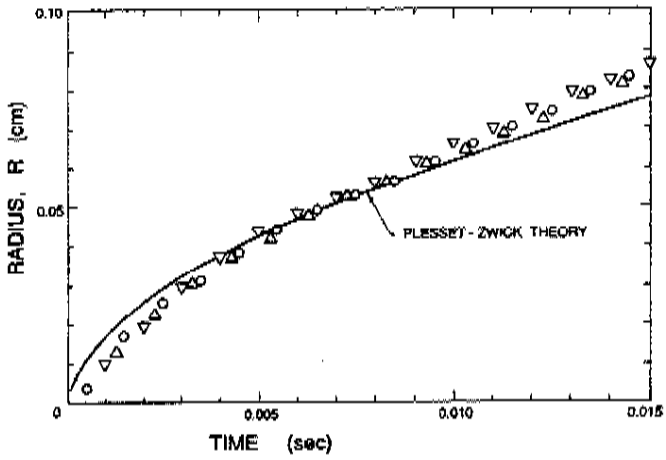

Figure 4.6. Experimental observations of the growth of three vapor bubbles (○, △, ▽) in superheated water at 103.1°C compared with the growth expected using the Plesset–Zwick theory (adapted from Dergarabedian 1953).

$(\mathcal{D}_L t)^{\frac{1}{2}}$, the Plesset–Zwick assumption remains valid indefinitely. An example of this thermally inhibited bubble growth is including in Figure 4.6, which is taken from Dergarabedian (1953). We observe that the experimental data and calculations using the Plesset–Zwick method agree quite well.

When bubble growth is caused by decompression so that $p_\infty(t)$ changes substantially with time during growth, the simple approximate solution of Eq. (4.48) no longer holds and the analysis of the unsteady thermal boundary layer surrounding the bubble becomes considerably more complex. One must then solve the diffusion Eq. (4.13), the energy equation [usually in the approximate form of Eq. (4.15)] and the Rayleigh–Plesset Eq. (4.10) simultaneously, though for the thermally controlled growth being considered here, most of the terms in Eq. (4.10) become negligible so that the simplification, $p_V(T_B) = p_\infty(t)$, is usually justified. When p_∞ is a constant this reduces to the problem treated by Plesset and Zwick (1952) and later addressed by Forster and Zuber (1954) and Scriven (1959). Several different approximate solutions to the general problem of thermally controlled bubble growth during liquid decompression have been put forward by Theofanous *et al.* (1969), Jones and Zuber (1978), and Cha and Henry (1981). All three analyses yield qualitatively similar results that also agree quite well with the experimental data of Hewitt and Parker (1968) for bubble growth in liquid nitrogen. Figure 4.7 presents a typical example of the data of Hewitt and Parker and a comparison with the three analytical treatments mentioned above.

Several other factors can complicate and alter the dynamics of thermally controlled growth. Nonequilibrium effects (Schrage 1953) can occur at very high evaporation rates where the liquid at the interface is no longer in thermal equilibrium with the vapor in the bubble and these have been explored by Theofanous *et al.* (1969) and

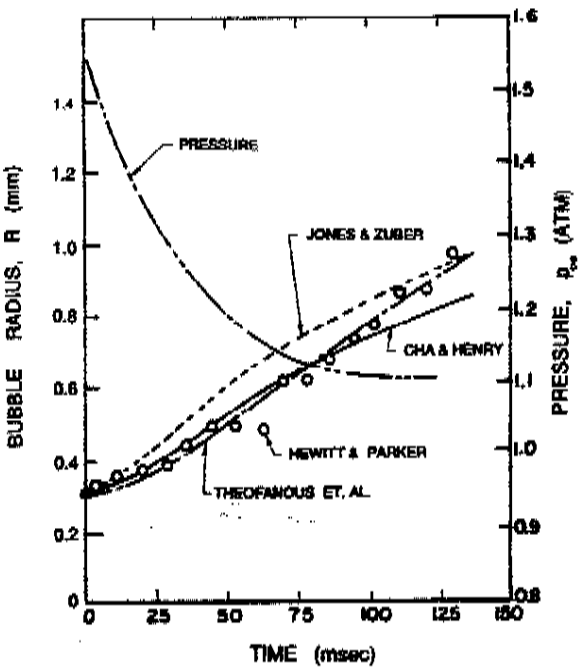

Figure 4.7. Data from Hewitt and Parker (1968) on the growth of a vapor bubble in liquid nitrogen (pressure/time history also shown) and comparison with the analytical treatments by Theofanous *et al.* (1969), Jones and Zuber (1978), and Cha and Henry (1981).

Plesset and Prosperetti (1977) among others. The consensus seems to be that this effect is insignificant except, perhaps, in some extreme circumstances. There is no clear indication in the experiments of any appreciable departure from equilibrium.

More important are the modifications to the heat transfer mechanisms at the bubble surface that may be caused by surface instabilities or by convective heat transfer. These are reviewed in Brennen (1995). Shepherd and Sturtevant (1982) and Frost and Sturtevant (1986) have examined rapidly growing nucleation bubbles near the limit of superheat and have found growth rates substantially larger than expected when the bubble was in the thermally controlled growth phase. Photographs (see Figure 4.8) reveal that the surfaces of those particular bubbles are rough and irregular. The enhancement of the heat transfer caused by this roughening is probably responsible

Figure 4.8. Typical photographs of a rapidly growing bubble in a droplet of superheated ether suspended in glycerine. The bubble is the dark, rough mass; the droplet is clear and transparent. The photographs, which are of different events, were taken 31, 44, and 58 μs after nucleation and the droplets are approximately 2 mm in diameter. Reproduced from Frost and Sturtevant (1986) with the permission of the authors.

for the larger than expected growth rates. Shepherd and Sturtevant (1982) attribute the roughness to the development of a baroclinic interfacial instability similar to the Landau–Darrieus instablity of flame fronts. In other circumstances, Rayleigh–Taylor instability of the interface could give rise to a similar effect (Reynolds and Berthoud 1981).

4.3.3 Cavitation and Boiling

The discussions of bubble dynamics in the last few sections lead, naturally, to two technologically important multiphase phenomena, namely cavitation and boiling. As we have delineated, the essential difference between cavitation and boiling is that bubble growth (and collapse) in boiling is inhibited by limitations on the heat transfer at the interface, whereas bubble growth (and collapse) in cavitation is limited not by heat transfer but only by inertial effects in the surrounding liquid. Cavitation is therefore an explosive (and implosive) process that is far more violent and damaging than the corresponding bubble dynamics of boiling. There are, however, many details that are relevant to these two processes and these are outlined in Chapters 5 and 6 respectively.

4.3.4 Bubble Growth by Mass Diffusion

In most of the circumstances considered in this chapter, it is assumed that the events occur too rapidly for significant mass transfer of contaminant gas to occur between the bubble and the liquid. Thus we assumed in Section 4.2.2 and elsewhere that the mass of contaminant gas in the bubble remained constant. It is convenient to reconsider this issue at this point, for the methods of analysis of mass diffusion will clearly be similar to those of thermal diffusion as described in Section 4.2.2 (see Scriven 1959). Moreover, there are some issues that require analysis of the rate of increase or decrease of the mass of gas in the bubble. One of the most basic issues is the fact that any and all of the gas-filled microbubbles that are present in a subsaturated liquid (and particularly in water) should dissolve away if the ambient pressure is sufficiently high. Henry's law states that the partial pressure of gas, p_{Ge}, in a bubble that is in equilibrium with a saturated concentration, c_∞, of gas dissolved in the liquid will be given by the following:

$$p_{Ge} = c_\infty \mathrm{He}, \tag{4.50}$$

where He is Henry's law constant for that gas and liquid combination (He decreases substantially with temperature). Consequently, if the ambient pressure, p_∞, is greater than $(c_\infty \mathrm{He} + p_V - 2S/R)$, the bubble should dissolve away completely. Experience is contrary to this theory, and microbubbles persist even when the liquid is subjected to several atmospheres of pressure for an extended period; in most instances, this stabilization of nuclei is caused by surface contamination.

The process of mass transfer can be analyzed by noting that the concentration, $c(r, t)$, of gas in the liquid will be governed by a diffusion equation identical in form to Eq. (4.13) as follows:

$$\frac{\partial c}{\partial t} + \frac{dR}{dt}\left(\frac{R}{r}\right)^2 \frac{\partial c}{\partial r} = \frac{D}{r^2}\frac{\partial}{\partial r}\left(r^2 \frac{\partial c}{\partial r}\right), \tag{4.51}$$

where D is the mass diffusivity, typically 2×10^{-5} cm^2/s for air in water at normal temperatures. As Plesset and Prosperetti (1977) demonstrate, the typical bubble growth rates due to mass diffusion are so slow that the convection term [the second term on the left-hand side of Eq. (4.51)] is negligible.

The simplest problem is that of a bubble of radius, R, in a liquid at a fixed ambient pressure, p_∞, and gas concentration, c_∞. In the absence of inertial effects the partial pressure of gas in the bubble will be p_{Ge} where

$$p_{Ge} = p_\infty - p_V + 2S/R \tag{4.52}$$

and therefore the concentration of gas at the liquid interface is $c_s = p_{Ge}/He$. Epstein and Plesset (1950) found an approximate solution to the problem of a bubble in a liquid initially at uniform gas concentration, c_∞, at time $t = 0$ that takes the following form:

$$R\frac{dR}{dt} = \frac{D}{\rho_G}\frac{\{c_\infty - c_s(1 + 2S/Rp_\infty)\}}{(1 + 4S/3Rp_\infty)}\left\{1 + R(\pi Dt)^{-\frac{1}{2}}\right\}, \tag{4.53}$$

where ρ_G is the density of gas in the bubble and c_s is the saturated concentration at the interface at the partial pressure given by Eq. (4.52) (the vapor pressure is neglected in their analysis). The last term in Eq. (4.53), $R(\pi Dt)^{-\frac{1}{2}}$, arises from a growing diffusion boundary layer in the liquid at the bubble surface. This layer grows like $(Dt)^{\frac{1}{2}}$. When t is large, the last term in Eq. (4.53) becomes small and the characteristic growth is given approximately by the following:

$$\{R(t)\}^2 - \{R(0)\}^2 \approx \frac{2D(c_\infty - c_s)t}{\rho_G}, \tag{4.54}$$

where, for simplicity, we have neglected surface tension.

It is instructive to evaluate the typical duration of growth (or shrinkage). From Eq. (4.54) the time required for complete solution is t_{cs} where

$$t_{cs} \approx \frac{\rho_G\{R(0)\}^2}{2D(c_s - c_\infty)}. \tag{4.55}$$

Typical values of $(c_s - c_\infty)/\rho_G$ are 0.01 (Plesset and Prosperetti 1977). Thus, in the absence of surface contaminant effects, a 10-μm bubble should completely dissolve in about 2.5 s.

Finally, we note that there is an important mass diffusion effect caused by ambient pressure oscillations in which nonlinearities can lead to bubble growth even in a subsaturated liquid. This is known as *rectified diffusion* and is discussed in Section 4.4.3.

4.4 Oscillating Bubbles

4.4.1 Bubble Natural Frequencies

In this and the sections that follow we consider the response of a bubble to oscillations in the prevailing pressure. We begin with an analysis of bubble natural frequencies in the absence of thermal effects and liquid compressibility effects. Consider the linearized dynamic solution of Eq. (4.25) when the pressure at infinity consists of a mean value, $\bar{p}_\infty$, upon which is superimposed a *small* oscillatory pressure of amplitude, $\tilde{p}$, and radian frequency, ω, so that

$$p_\infty = \bar{p}_\infty + \mathrm{Re}\{\tilde{p}e^{j\omega t}\}. \tag{4.56}$$

The linear dynamic response of the bubble is represented by the following:

$$R = R_e[1 + \mathrm{Re}\{\varphi e^{j\omega t}\}], \tag{4.57}$$

where R_e is the equilibrium size at the pressure $\bar{p}_\infty$ and the bubble radius response, φ, will in general be a complex number such that $R_e|\varphi|$ is the amplitude of the bubble radius oscillations. The phase of φ represents the phase difference between p_∞ and R.

For the present we assume that the mass of gas in the bubble, m_G, remains constant. Then substituting Eqs. (4.56) and (4.57) into Eq. (4.25), neglecting all terms of order $|\varphi|^2$ and using the equilibrium condition of Eq. (4.37), one finds the following:

$$\omega^2 - j\omega\frac{4\nu_L}{R_e^2} + \frac{1}{\rho_L R_e^2}\left\{\frac{2S}{R_e} - 3kp_{Ge}\right\} = \frac{\tilde{p}}{\rho_L R_e^2 \varphi}, \tag{4.58}$$

where, as before,

$$p_{Ge} = \bar{p}_\infty - p_V + \frac{2S}{R_e} = \frac{3m_G T_B \mathcal{R}_G}{4\pi R_e^3}. \tag{4.59}$$

It follows that for a given amplitude, $\tilde{p}$, the maximum or peak response amplitude occurs at a frequency, ω_p, given by the minimum value of the spectral radius of the left-hand side of Eq. (4.58):

$$\omega_p = \left\{\frac{(3kp_{Ge} - 2S/R_e)}{\rho_L R_e^2} - \frac{8\nu_L^2}{R_e^4}\right\}^{\frac{1}{2}} \tag{4.60}$$

or in terms of $(\bar{p}_\infty - p_V)$ rather than p_{Ge}:

$$\omega_p = \left\{\frac{3k(\bar{p}_\infty - p_V)}{\rho_L R_e^2} + \frac{2(3k-1)S}{\rho_L R_e^3} - \frac{8\nu_L^2}{R_e^4}\right\}^{\frac{1}{2}}. \tag{4.61}$$

At this peak frequency the amplitude of the response is, of course, inversely proportional to the damping as follows:

$$|\varphi|_{\omega=\omega_p} = \frac{\tilde{p}}{4\mu_L\{\omega_p^2 + \frac{4\nu_L^2}{R_e^4}\}^{\frac{1}{2}}}. \tag{4.62}$$

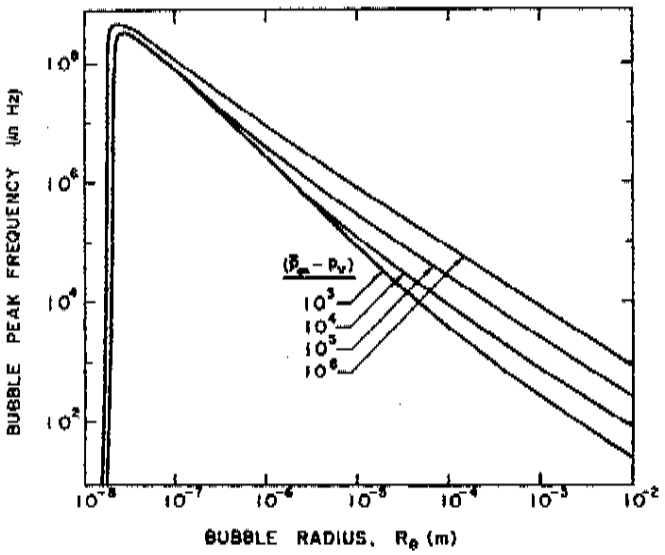

Figure 4.9. Bubble resonant frequency in water at 300°K ($S = 0.0717$, $\mu_L = 0.000863$, $\rho_L = 996.3$) as a function of the radius of the bubble for various values of $(\bar{p}_\infty - p_V)$ as indicated.

It is also convenient for future purposes to define the natural frequency, ω_n, of oscillation of the bubbles as the value of ω_p for zero damping:

$$\omega_n = \left\{ \frac{1}{\rho_L R_e^2} \left\{ 3k(\bar{p}_\infty - p_V) + 2(3k-1)\frac{S}{R_e} \right\} \right\}^{\frac{1}{2}}. \tag{4.61}$$

The connection with the stability criterion of Section 4.2.5 is clear when one observes that no natural frequency exists for tensions $(p_V - \bar{p}_\infty) > 4S/3R_e$ (for isothermal gas behavior, $k = 1$); stable oscillations can only occur about a stable equilibrium.

Note from Eq. (4.61) that ω_p is a function only of $(\bar{p}_\infty - p_V)$, R_e, and the liquid properties. A typical graph for ω_p as a function of R_e for several $(\bar{p}_\infty - p_V)$ values is shown in Figure 4.9 for water at 300°K ($S = 0.0717$, $\mu_L = 0.000863$, $\rho_L = 996.3$). As is evident from Eq. (4.61), the second and third terms on the right-hand side dominate at very small R_e and the frequency is almost independent of $(\bar{p}_\infty - p_V)$. Indeed, no peak frequency exists below a size equal to about $2\nu_L^2\rho_L/S$. For larger bubbles the viscous term becomes negligible and ω_p depends on $(\bar{p}_\infty - p_V)$. If the latter is positive, the natural frequency approaches zero like R_e^{-1}. In the case of tension, $p_V > \bar{p}_\infty$, the peak frequency does not exist above $R_e = R_c$.

For typical nuclei found in water (1 to 100 μm) the natural frequencies are of the order of 5 to 25 kHz. This has several important practical consequences. First, if one wishes to cause cavitation in water by means of an imposed acoustic pressure field, then the frequencies that will be most effective in producing a substantial concentration of large cavitation bubbles will be in this frequency range. This is also the frequency range employed in magnetostrictive devices used to oscillate solid material samples in water (or other liquid) to test the susceptibility of that material to cavitation damage

(Knapp *et al.* 1970). Of course, the oscillation of the nuclei produced in this way will be highly nonlinear and therefore peak response frequencies will be significantly lower than those given above.

There are two important footnotes to this linear dynamic analysis of an oscillating bubble. First, the assumption that the gas in the bubble behaves polytropically is a dubious one. Prosperetti (1977) has analyzed the problem in detail with particular attention to heat transfer in the gas and has evaluated the effective polytropic exponent as a function of frequency. Not surprisingly the polytropic exponent increases from unity at very low frequencies to γ at intermediate frequencies. However, more unexpected behaviors develop at high frequencies. At the low and intermediate frequencies, the theory is largely in agreement with Crum's (1983) experimental measurements. Prosperetti, Crum, and Commander (1988) provide a useful summary of the issue.

A second, related concern is the damping of bubble oscillations. Chapman and Plesset (1971) presented a summary of the three primary contributions to the damping of bubble oscillations, namely that due to liquid viscosity, that due to liquid compressibility through acoustic radiation, and that due to thermal conductivity. It is particularly convenient to represent the three components of damping as three additive contributions to an effective liquid viscosity, μ_e, that can then be employed in the Rayleigh–Plesset equation in place of the actual liquid viscosity, μ_L:

$$\mu_e = \mu_L + \mu_t + \mu_a \tag{4.64}$$

where the *acoustic* viscosity, μ_a, is given by the following:

$$\mu_a = \frac{\rho_L \omega^2 R_e^2}{4c_L}, \tag{4.65}$$

where c_L is the velocity of sound in the liquid. The *thermal* viscosity, μ_t, follows from the analysis by Prosperetti (1977) mentioned in the previous paragraph (see also Brennen 1995). The relative magnitudes of the three components of damping (or *effective* viscosity) can be quite different for different bubble sizes or radii, R_e. This is illustrated by the data for air bubbles in water at 20°C and atmospheric pressure that is taken from Chapman and Plesset (1971) and reproduced as Figure 4.10.

4.4.2 Nonlinear Effects

Due to the nonlinearities in the governing equations, particularly the Rayleigh–Plesset Eq. (4.10), the response of a bubble subjected to pressure oscillations will begin to exhibit important nonlinear effects as the amplitude of the oscillations is increased. In the last few sections of this chapter we briefly review some of these nonlinear effects. Much of the research appears in the context of acoustic cavitation, a subject with an extensive literature that is reviewed in detail elsewhere (Flynn 1964, Neppiras 1980; Plesset and Prosperetti 1977, Prosperetti 1982, 1984, Crum 1979, Young 1989). We include here a brief summary of the basic phenomena.

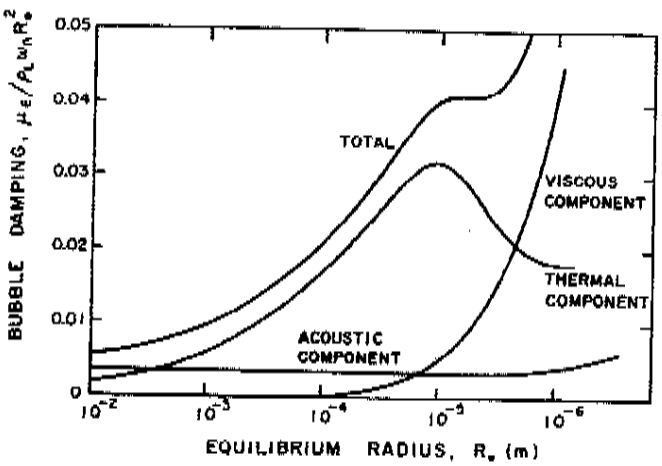

Figure 4.10. Bubble damping components and the total damping as a function of the equilibrium bubble radius, R_e, for water. Damping is plotted as an *effective* viscosity, μ_e, nondimensionalized as shown (from Chapman and Plesset 1971).

As the amplitude increases, the bubble *may* continue to oscillate stably. Such circumstances are referred to as *stable acoustic cavitation* to distinguish them from those of the *transient* regime described below. Several different nonlinear phenomena can affect stable acoustic cavitation in important ways. Among these are the production of subharmonics, the phenomenon of rectified diffusion (see Section 4.4.3) and the generation of Bjerknes forces (see Section 3.4). At larger amplitudes the change in bubble size during a single period of oscillation can become so large that the bubble undergoes a cycle of explosive cavitation growth and violent collapse similar to that described earlier in the chapter. Such a response is termed *transient acoustic cavitation* and is distinguished from stable acoustic cavitation by the fact that the bubble radius changes by several orders of magnitude during each cycle.

As Plesset and Prosperetti (1977) have detailed in their review of the subject, when a liquid that will inevitably contain microbubbles is irradiated with sound of a given frequency, ω, the nonlinear response results in harmonic dispersion that produces not only harmonics with frequencies that are integer multiples of ω (superharmonics) but, more unusually, subharmonics with frequencies less than ω of the form $m\omega/n$, where m and n are integers. Both the superharmonics and subharmonics become more prominent as the amplitude of excitation is increased. The production of subharmonics was first observed experimentally by Esche (1952), and possible origins of this nonlinear effect were explored in detail by Noltingk and Neppiras (1950, 1951), Flynn (1964), Borotnikova and Soloukin (1964), and Neppiras (1969), among others. Lauterborn (1976) examined numerical solutions for a large number of different excitation frequencies and was able to demonstrate the progressive development of the peak responses at subharmonic frequencies as the amplitude of the excitation is increased. Nonlinear effects not only create these subharmonic peaks but also cause the resonant peaks to be shifted to lower frequencies, creating discontinuities that correspond to bifurcations in the solutions. The weakly nonlinear

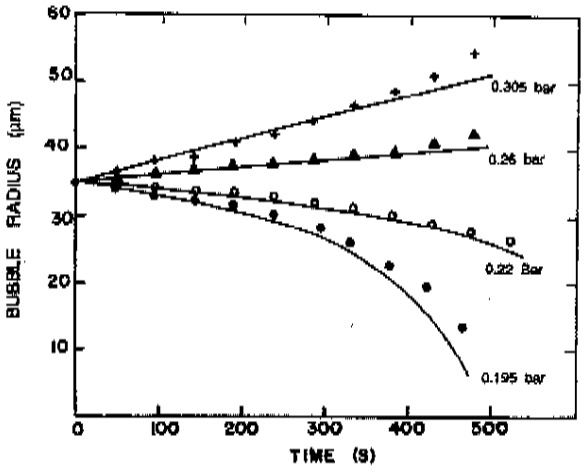

Figure 4.11. Examples from Crum (1980) of the growth (or shrinkage) of air bubbles in saturated water ($S = 68$ dynes/cm) due to rectified diffusion. Data is shown for four pressure amplitudes as shown. The lines are the corresponding theoretical predictions.

analysis of Brennen (1995) produces similar phenomena. In recent years, the modern methods of nonlinear dynamical systems analysis have been applied to this problem by Lauterborn and Suchla (1984), Smereka, Birnir, and Banerjee (1987), Parlitz *et al.* (1990), and others and have led to further understanding of the bifurcation diagrams and strange attractor maps that arise in the dynamics of single bubble oscillations.

Finally, we comment on the phenomenon of transient cavitation in which a phase of explosive cavitation growth and collapse occurs each cycle of the imposed pressure oscillation. We seek to establish the level of pressure oscillation at which this will occur, known as the threshold for transient cavitation (see Noltingk and Neppiras 1950, 1951, Flynn 1964, Young 1989). The answer depends on the relation between the radian frequency, ω, of the imposed oscillations and the natural frequency, ω_n, of the bubble. If $\omega \ll \omega_n$, then the liquid inertia is relatively unimportant in the bubble dynamics and the bubble will respond quasistatically. Under these circumstances the Blake criterion [see Section 4.2.5, Eq. (4.41)] will hold and the critical conditions will be reached when the minimum instantaneous pressure just reaches the critical Blake threshold pressure. On the other hand, if $\omega \gg \omega_n$, the issue will involve the dynamics of bubble growth since inertia will determine the size of the bubble perturbations. The details of this bubble dynamic problem have been addressed by Flynn (1964) and convenient guidelines are provided by Apfel (1981).

4.4.3 Rectified Mass Diffusion

When a bubble is placed in an oscillating pressure field, an important nonlinear effect can occur in the mass transfer of dissolved gas between the liquid and the bubble. This effect can cause a bubble to grow in response to the oscillating pressure when it would not otherwise do so. This effect is known as *rectified mass diffusion* (Blake 1949) and is important because it may cause nuclei to grow from a stable size to an unstable size and thus provide a supply of cavitation nuclei. Analytical models of the phenomenon were first put forward by Hsieh and Plesset (1961) and Eller and

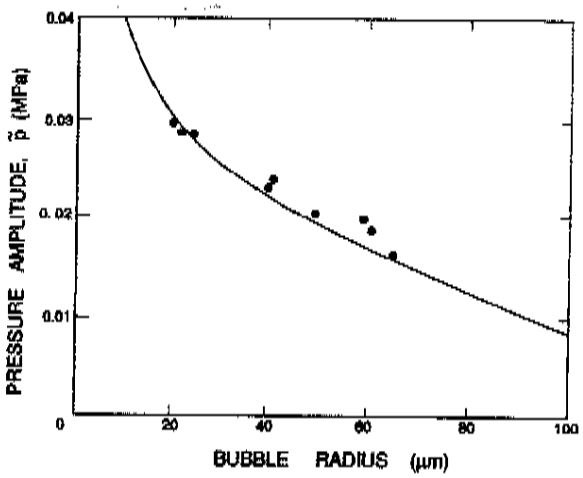

Figure 4.12. Data from Crum (1984) of the threshold pressure amplitude for rectified diffusion for bubbles in distilled water ($S = 68$ dynes/cm) saturated with air. The frequency of the sound is 22.1 kHz. The line is the theoretical prediction.

Flynn (1965), and reviews of the subject can be found in Crum (1980, 1984) and Young (1989).

Consider a gas bubble in a liquid with dissolved gas as described in Section 4.3.4. Now, however, we add an oscillation to the ambient pressure. Gas will tend to come out of solution into the bubble during that part of the oscillation cycle when the bubble is larger than the mean because the partial pressure of gas in the bubble is then depressed. Conversely, gas will redissolve during the other half of the cycle when the bubble is smaller than the mean. The linear contributions to the mass of gas in the bubble will, of course, balance so that the average gas content in the bubble will not be affected at this level. However, there are two nonlinear effects that tend to increase the mass of gas in the bubble. The first of these is due to the fact that release of gas by the liquid occurs during that part of the cycle when the surface area is larger, and therefore the influx during that part of the cycle is slightly larger than the efflux during the part of the cycle when the bubble is smaller. Consequently, there is a net flux of gas into the bubble that is quadratic in the perturbation amplitude. Second, the diffusion boundary layer in the liquid tends to be stretched thinner when the bubble is larger, and this also enhances the flux into the bubble during the part of the cycle when the bubble is larger. This effect contributes a second, quadratic term to the net flux of gas into the bubble.

Strasberg (1961) first explored the issue of the conditions under which a bubble would grow due to rectified diffusion. This and later analyses showed that, when an oscillating pressure is applied to a fluid consisting of a subsaturated or saturated liquid and seeded with microbubbles of radius R_e, there will exist a certain critical or threshold amplitude above which the microbubbles will begin to grow by rectified diffusion. The analytical expressions for the rate of growth and for the threshold pressure amplitudes agree quite well with the corresponding experimental measurements for distilled water saturated with air made by Crum (1980, 1984) (see Figures 4.11 and 4.12).